

This discussion paper is/has been under review for the journal Atmospheric Chemistry and Physics (ACP). Please refer to the corresponding final paper in ACP if available.

Smoke injection heights from agricultural burning in Eastern Europe as seen by CALIPSO

V. Amiridis¹, E. Giannakaki², D. S. Balis², E. Gerasopoulos³, I. Pytharoulis⁴, P. Zanis⁴, S. Kazadzis³, D. Melas², and C. Zerefos⁵

¹Institute for Space Applications and Remote Sensing, National Observatory of Athens, Athens, 15236, Greece

²Laboratory of Atmospheric Physics, Aristotle University of Thessaloniki, Thessaloniki, Greece

³Institute for Environmental Research and Sustainable Development, National Observatory of Athens, Athens, 15236, Greece

⁴Department of Meteorology and Climatology, Aristotle University of Thessaloniki, Thessaloniki, Greece

⁵Laboratory of Climatology, University of Athens, Athens, Greece

Received: 15 July 2010 – Accepted: 9 August 2010 – Published: 16 August 2010

Correspondence to: V. Amiridis (vamoir@space.noa.gr)

Published by Copernicus Publications on behalf of the European Geosciences Union.

Smoke injection heights from agricultural burning in Eastern Europe

V. Amiridis et al.

Title Page

Abstract

Introduction

Conclusions

References

Tables

Figures

⏪

⏩

◀

▶

Back

Close

Full Screen / Esc

Printer-friendly Version

Interactive Discussion

Abstract

High frequency of agricultural fires is observed every year during the summer months over SW Russia and Eastern Europe. This study investigates the initial injection height of aerosol generated by the fires over these regions during the biomass burning season, which determines the potential for long-range transport of the smoke. This information is critical for aerosol transport modeling, as it determines the smoke plume evolution. The study focuses on the period 2006–2008, and is based on observations made by the CALIOP instrument on board the NASA CALIPSO satellite. MODIS data are synergistically used for the detection of the fires and the characterization of their intensity. CALIPSO aerosol vertical distributions generated by the active fires are analyzed to investigate the aerosol top height which is considered dependent on the heat generated by the fires and can be associated with the initial injection height. Aerosol top heights of the vertically homogenous smoke layers are found to range between 1.6 and 5.9 km. Smoke injection heights from CALIPSO are compared with mixing layer heights taken by the European Centre for Medium-range Weather Forecast (ECMWF), to investigate the direct injection of smoke particles to the free troposphere. Our results indicate that the aerosol plumes are observed within the boundary layer for the 50% of the cases examined. For the rest of the cases, the strong updrafts generated by the fires resulted to smoke injection heights greater than the ECMWF estimated mixing layer by 0.5 to 3.0 km, indicating a direct smoke injection into the free troposphere. The smoke injection height showed a dependence on the MODIS-Land Fire Radiative Power product which is indicative of the fire intensity.

1 Introduction

Giglio et al. (2003), investigating the spatial and temporal occurrence of fires in croplands, based on the Moderate Resolution Imaging Spectroradiometer (MODIS) active fire product, showed that the Russian Federation was the largest contributor to agricultural burning globally during the period 2001 to 2003, producing 31–36% of all

Smoke injection heights from agricultural burning in Eastern Europe

V. Amiridis et al.

Title Page

Abstract

Introduction

Conclusions

References

Tables

Figures

⏪

⏩

◀

▶

Back

Close

Full Screen / Esc

Printer-friendly Version

Interactive Discussion



agricultural fires. This globally highest concentration of agricultural fires, found to be extended across Russia in the latitudinal belt between 45° N–55° N during spring (April–May), as well as in Eastern Europe (Baltic countries, western Russia, Belarus, and the Ukraine) during late summer (end of July and August). Forest fires in this area are a major source of pollution in the Northern Hemisphere and especially Europe (Korontzi et al., 2006). Moreover, areas downwind of those fires (e.g. Eastern Mediterranean) are characterized by enhanced particulate loadings in the column but also at surface, especially during summer when meteorology favors the transport from northerly directions (e.g. Balis et al., 2003; Gerasopoulos et al., 2003, 2006; Amiridis et al., 2005; Fotiadi et al., 2006; Amiridis et al., 2009; Kazadzis et al., 2009), thus the need to model smoke transport and estimate its contribution to air quality degradation is important.

Smoke injection heights are key inputs for aerosol transport modeling, as they are critical for determining the distance and direction of the travelling smoke (e.g., Colarco et al., 2004; Freitas et al., 2007). Biomass burning emits hot gases and particles, which are transported upward due to positive buoyancy. The interaction between the smoke and the environment produces eddies that entrain colder environmental air into the smoke plume, which dilutes the plume and reduces buoyancy. The final plume height is mostly controlled by the thermodynamic stability of the ambient atmosphere and the fire intensity. After this initial injection phase, the smoke enters the general atmospheric circulation. The fraction that is within the planetary boundary layer (PBL) height is well mixed by turbulent eddies and the particles experience more efficient removal processes than in the free troposphere (scavenging and wet-removal). On the other hand, the fraction of smoke that reaches the free troposphere is advected away faster from the source region while the residence time of the particles at these heights is increased. The described mechanism has a strong impact on pollutant dispersion, and as a consequence, the information of the initial injection height, and whether it appears inside the PBL or above, is a major parameter for a proper understanding and modeling of the atmospheric chemistry and transport of smoke (e.g. Freitas et al., 2007).

Smoke injection heights from agricultural burning in Eastern Europe

V. Amiridis et al.

[Title Page](#)[Abstract](#)[Introduction](#)[Conclusions](#)[References](#)[Tables](#)[Figures](#)[⏪](#)[⏩](#)[◀](#)[▶](#)[Back](#)[Close](#)[Full Screen / Esc](#)[Printer-friendly Version](#)[Interactive Discussion](#)

area by means of biomass burning frequency and intensity, downwind of which severe air quality degradation is already encountered (e.g. Lelieveld et al., 2002). Finally, we attempted to assess the contribution of fires to the injection of smoke above the PBL by calculating the distribution of differences between aerosol injection height derived from CALIPSO, and PBL height obtained from the European Centre for Medium-range Weather Forecasts (ECMWF).

2 Data and methodology

2.1 MODIS active fire

For the identification of the areas that are affected by biomass burning over Western Russia and Eastern Europe during the biomass burning season, the MODIS active fire product (Giglio et al., 2003) has been used. The MODIS sensor is a multi-spectral sensor with 36 spectral bands, ranging in wavelength from 0.4 to 14.2 μm , and fires are detected at 1 km spatial resolution (at nadir) using radiance measurements in the 4 μm and 11 μm channels. Measurements at several spectral bands are utilized for masking clouds, extremely bright surfaces, glint, and other potential sources of false alarms (Giglio et al., 2003). In the operational MODIS algorithm, only the 4 μm channel measurements are used to calculate the Fire Radiative Power (FRP), based on the measured brightness temperatures of the fire pixel and its neighboring surface background. There are two 4 μm channels on each MODIS sensor, one of which is a “low-gain” channel that can record pixel-integrated brightness temperatures of up to ~ 500 K, thereby allowing unsaturated measurements to be made over even very large/most intensely burning wildfires. MODIS is a twin sensor flying on two NASA Earth Observing System (EOS) satellites: Terra (launched 19 December 1999) and Aqua (launched 4 May 2002). They are both polar orbiting, with Terra crossing the equator at approximately 10:30 a.m. and 10:30 p.m. local time, and Aqua at approximately 1:30 a.m. and 1:30 p.m. local time. Each MODIS sensor achieves near-global

Smoke injection heights from agricultural burning in Eastern Europe

V. Amiridis et al.

Title Page

Abstract

Introduction

Conclusions

References

Tables

Figures

⏪

⏩

◀

▶

Back

Close

Full Screen / Esc

Printer-friendly Version

Interactive Discussion



coverage once per day and once per night every 24 h, with higher latitude locations observed slightly more frequently because of increasingly large overlaps from successive satellite passes. Therefore, most fires detectable at a 1 km spatial resolution have the potential to have their FRP measured four times a day, except when covered by thick meteorological cloud. MODIS algorithms (including the fire algorithm) are updated periodically, leading to different versions, which are used to generate a series of Collections of the data products. The latest “Collection 5” fire data were used in this study.

2.2 CALIPSO

The Cloud-Aerosol Lidar and Infrared Pathfinder Satellite Observation (CALIPSO) mission is a collaborative effort between the NASA Langley Research Center (LaRC), the Centre National D’Etudes Spatiales (CNES), Hampton University (HU), the Institut Pierre Simon Laplace (IPSL), and Ball Aerospace and Technologies Corporation (BATC) to study global radiative effects of aerosols and clouds on climate. CALIPSO is an Earth Science observation mission that launched on 28 April 2006 and flies in nominal orbital altitude of 705 km and an inclination of 98 degrees as part of a constellation of Earth-observing satellites including Aqua, PARASOL, and Aura—collectively known as the “A-train”. The CALIPSO mission provides crucial lidar and passive sensors to obtain unique data on aerosol and cloud vertical structure and optical properties (Winker et al., 2007).

CALIPSO’s lidar, the Cloud-Aerosol Lidar with Orthogonal Polarization (CALIOP), is an elastically backscattered lidar operating at 532 and 1064 nm, equipped with a depolarization channel at 532 nm that provides high-resolution vertical profiles of aerosols and clouds. The lasers operate at 20.16 Hz and are Q-switched to provide a pulse length of about 20 ns. Each laser generates nominally 220 mJ per pulse at 1064 nm, which is frequency-doubled to produce about 110 mJ of pulse energy at each of the two wavelengths. Beam expanders reduce the angular divergence of the transmitted laser beam to produce a beam diameter of 70 m at the Earth’s surface (corresponding

Smoke injection heights from agricultural burning in Eastern Europe

V. Amiridis et al.

Title Page

Abstract

Introduction

Conclusions

References

Tables

Figures

⏪

⏩

◀

▶

Back

Close

Full Screen / Esc

Printer-friendly Version

Interactive Discussion



Discussion Paper | Discussion Paper | Discussion Paper | Discussion Paper | Discussion Paper

to a nominal laser beam divergence of 100 μ rad) (Winker et al., 2004, 2006, 2007).

CALIPSO produces Level 1 and Level 2 scientific data products. The Level 1 data include: lidar calibrated and geolocated profiles with associated browse imagery with horizontal resolutions of 1/3 km, 1 km and 5 km, an aerosol layer product at 5 km resolution (height, thickness, optical depth, and integrated attenuated backscatter), and an aerosol profile product with a horizontal resolution of 40 km and vertical resolution of 120 m (backscatter, extinction, and depolarization ratio). CALIPSO Level-2 aerosol layer product provides a description of the aerosol layers, including their top heights and bottoms, identified by the use of automated algorithms from the Level-1 data. Detailed description of the abovementioned algorithms is given in Vaughan et al., 2004 and Winker et al., 2009. However, Level 2, version 2.01 release of this product “contains a number of errors and/or inconsistencies” (see respective CALIPSO data quality statement, http://eosweb.larc.nasa.gov/PRODOCS/calipso/Quality_Summaries/CALIOP_L2ProfileProducts_2.01.html). The newly released version 3.01 of the Level 2 CALIPSO product features a comprehensive restructuring and expansion of the Lidar Level 2 cloud and aerosol profile products, significant enhancements to the Lidar Level 2 cloud and aerosol profile products and the implementation of an improved calibration technique for the Lidar Level 1 532 nm day-time calibration (http://eosweb.larc.nasa.gov/PRODOCS/calipso/Quality_Summaries/). Even though all studies to date indicate acceptable performance of this product, the status of derived products from this second class of algorithms remains Provisional. All obvious artifacts have been identified and corrected in these data, but only limited comparisons with independent data sets are currently available.

2.3 ECMWF mixing layer height

Mixing layer height analyses were retrieved from the ECMWF model that provides a diagnostic of the boundary layer height with a 12-hourly and $0.25^\circ \times 0.25^\circ$ latitude-longitude resolution. The height of the model topography is added to the grid-point

Smoke injection heights from agricultural burning in Eastern Europe

V. Amiridis et al.

Title Page

Abstract

Introduction

Conclusions

References

Tables

Figures



Back

Close

Full Screen / Esc

Printer-friendly Version

Interactive Discussion



values in order to make them comparable to the satellite data that provide heights above sea-level. The boundary layer height at a specific location is calculated through bilinear interpolation, using the weighted values of the four surrounding grid-points. As expected, the 12-hourly fields show a strong diurnal cycle with low values at night.

5 The parameterization of the mixed layer (and entrainment) in the deterministic atmospheric model of ECMWF uses a boundary layer height from an entraining parcel model (ECMWF, 2009b). The bulk Richardson method (Troen and Mahrt, 1986) is used as a diagnostic, independent of the turbulence parameterization, in order to get a continuous field also in neutral and stable conditions. The boundary layer height is the
10 level where the bulk Richardson number, based on the properties of that level and the lowest model level, reaches the critical value of 0.25. If it is found to be between two model levels, the exact height is calculated through linear interpolation. It is noted that during the period of interest (2006–2008) the ECMWF model used 91 vertical levels up to 0.01 hPa, with a high vertical resolution in the boundary layer (approximately 14
15 hybrid levels in the lowest 150 hPa).

The boundary layer height analyses of the operational early-delivery assimilation system of ECMWF are utilized in this study. This system consists of two 6 h 4D-Var analysis cycles, at 00:00 and 12:00 UTC. The 00:00 UTC (12:00 UTC) cycle uses observations from the time window 21:01–03:00 UTC (09:01–15:00 UTC) and a first
20 guess forecast from the 12:00 UTC (00:00 UTC) delayed-cut-off 12 h 4D-Var analysis of the previous (same) day (Haseler, 2004). The deterministic and ensemble prediction forecasts of ECMWF are initialized from the analyses of the early-delivery system (Persson and Grazzini, 2005). Haseler (2004) showed that the quality of the two first
25 guesses is sufficiently high to allow the functioning of the abovementioned operational assimilation system without compromising the quality of the model forecasts.

A very large amount of observations from various sources is introduced in the data assimilation system. Typically, before the quality control there is a total of 75 million pieces of data available worldwide, around 98% from satellites, in a 12 h period (Persson and Grazzini, 2005). These data are divided into surface observations, upper-air

Smoke injection heights from agricultural burning in Eastern Europe

V. Amiridis et al.

Title Page

Abstract

Introduction

Conclusions

References

Tables

Figures



Back

Close

Full Screen / Esc

Printer-friendly Version

Interactive Discussion



observations from radiosondes and aircrafts, and satellite observations (mainly radiances) (ECMWF 2009a).

3 Results and discussion

3.1 Description of fires and prevailing meteorological conditions

5 For the detection of fires for the fire season periods (July and August) between 2006 and 2008, the MODIS fire product over a grid extended to the longitudinal belt between 25° to 45° E, and the latitudinal belt between 40° to 60° N has been used. Amiridis et al. (2009), used a global land cover classification with a resolution of 300 m to show that the detected fires in the area of the abovementioned grid are mainly associated with agricultural burning activities. The locations of the active fires identified from MODIS observations are presented in Fig. 1 (crosses). For the same period, the CALIPSO overpasses are superimposed. From the analysis of the FRP product of MODIS for the fires presented in Fig. 1, the overall minimum and maximum values of the FRP per pixel (1 × 1 km) detected by the sensor for the period under study (2006–2008),
10 ranged between 11.36 to 438.71 MW with a mean value of 50.23 ± 57 MW. FRP values reported here refer to fires with MODIS fire detection confidence greater than 80%. The detection confidence, which varies between 0 and 100%, is a heuristic measure of the radiometric contrast between a fire pixel and its immediate non-fire neighborhood, with extra penalties imposed near potential false alarm sources such as cloud edges and coastline (Giglio et al., 2003). Following the same criteria, Ichoku et al. (2008),
15 based on a 1 km resolution data of FRP acquired globally by the MODIS sensor from 2000 to 2006, showed that instantaneous FRP values ranged between 0.02 MW and 1866 MW, with Indochina and the African regions portray the highest peaks. Following the categorization of fire strength of Ichoku et al. (2008), the fires presented here fall
20 within category 1 and 2. According to the same study, only less than 1% of the total fires globally fall into each of categories 3 to 5.

Smoke injection heights from agricultural burning in Eastern Europe

V. Amiridis et al.

Title Page

Abstract

Introduction

Conclusions

References

Tables

Figures



Back

Close

Full Screen / Esc

Printer-friendly Version

Interactive Discussion



Smoke injection heights from agricultural burning in Eastern Europe

V. Amiridis et al.

Title Page

Abstract

Introduction

Conclusions

References

Tables

Figures

⏪

⏩

◀

▶

Back

Close

Full Screen / Esc

Printer-friendly Version

Interactive Discussion



The fires presented in this paper are of agricultural nature, and thus common practices are followed by the farmers including the fact that no fires are lit in times of strong or gusty winds. These measures are applied to control the lighting of the fires, as the fire danger is high during the summer fire season and may result to uncontrolled situations, especially during unsettled weather conditions. This is evident for the fires detected in the study area (Fig. 1) if we consider the respective ECMWF wind speed data (Fig. 2). The average wind speed at 850 hPa is found equal to 7.0 ± 3.5 m/sec, varying from 0.3 to 23 m/sec, with the 86% of the values below 10 m/sec. These data indicate weak to moderate horizontal winds resulting in relatively slow advection of smoke plumes for the fires examined here, and this is rational since agricultural fires set by farmers are chosen during low wind speed to maintain control of the fire. From the analysis of the CALIPSO aerosol vertical profiles examined in this study, no significant vertical variability is observed (see for example Fig. 3), indicating strong convection over the fire pixel and homogeneous smoke concentrations with height. Thus, in our case it may be assumed that horizontal advection poses no or slight impact to the height that smoke is injected in to the atmosphere.

3.2 CALIPSO retrieval of smoke injection height

Due to the limitations presented in the methodology Sect. 2.2 considering CALIPSO Level 2 product, much caution is required in the use and analysis of their aerosol top layer height. The detection of the mixing layer by an automated algorithm is not easy to implement and can be associated with considerable errors, e.g., if the signal intensity is low and large statistical fluctuations cause sharp gradients in the profile. Such an algorithm requires the definition of threshold values (see Winker et al., 2009) and the results also depend on data averaging and spatial resolution of the range-corrected signals. Therefore, for the needs of the current study, smoke injection heights are directly calculated from Level 1 attenuated backscatter profiles at 532 nm by applying a slope method (Pal et al., 1992) on each individual profile. In the application of the slope method, the steep gradient in the attenuated backscatter signal – resulting from the

high decrease in attenuated aerosol backscatter caused by lower particle concentration and humidity above the mixing layer – has been identified in the lidar profiles. The method is very simple and it has been used since many years (Flamant et al., 1997; Menut et al., 1999). It is also validated against independent methods to derive the mixing height (e.g. Kaimal et al., 1982) showing good agreement under well mixed conditions.

Time coincidence of CALIPSO and MODIS data is only possible for the MODIS instrument aboard Aqua satellite, since in that case the time difference between the overpasses is of the order of 75 s, with Aqua preceding the CALIPSO satellite. CALIPSO shots are then averaged within the MODIS pixel to produce the MODIS-located lidar profile. The resulted profile can be very noisy, especially during daytime acquisitions, allowing only poor retrievals of layer products using the slope method. While high signal to noise ratio (SNR) is required for the slope method to function properly, CALIPSO's orbital velocity of ~7 km/sec combined with the need to retrieve feature boundaries of the aerosol layers at high vertical and horizontal resolutions allows only minimal spatial averaging. To overcome SNR constrains, a 5 km spatial averaging centered in the MODIS (1 × 1 km) fire pixel has been applied in addition to vertical moving average at a window frame of 400 m. Following our approach, the collocation could be highly inaccurate under these assumptions, giving false results when MODIS products are compared with CALIPSO ones. However, no significant changes have been found on the shape of aerosol layers between the correctly collocated 1 km horizontally averaged CALIPSO profiles and the 5 km profiles centered in the MODIS pixel. This can be attributed to the possible horizontal distribution of smoke around the fire pixel for our cases, or to the existence of fire pixels in an area extended on the neighbour of the fire pixel under study, resulting in dispersed smoke in a wide area over the CALIPSO overpass.

To compare our approach with CALIPSO's algorithm aerosol layer Level 2 (Version 2.01) retrievals and to additionally demonstrate our methodology for the calculation of smoke injection heights, we present two examples from our dataset in Fig. 3. In

Smoke injection heights from agricultural burning in Eastern Europe

V. Amiridis et al.

Title Page

Abstract

Introduction

Conclusions

References

Tables

Figures



Back

Close

Full Screen / Esc

Printer-friendly Version

Interactive Discussion



Smoke injection heights from agricultural burning in Eastern Europe

V. Amiridis et al.

Title Page

Abstract

Introduction

Conclusions

References

Tables

Figures



Back

Close

Full Screen / Esc

Printer-friendly Version

Interactive Discussion



both examples, the vertical profile of the CALIPSO attenuated backscatter coefficient at 532 nm (horizontally averaged at 5 km), are centered in the MODIS pixel. Additionally, the bottom and top heights of the aerosol layers detected by CALIPSO's Level 2 (Version 2.01) product are presented with horizontal lines. In the first case of 15 August 2006 (Fig. 3a), the aerosol layer is well captured by CALIPSO algorithm and the Level-2 automatic calculations are consistent with the results of our slope method, giving an aerosol top height of the order of 2700 m. Following our method, the minimum of the derivative (right panel) is considered as the smoke injection height for the fire pixels detected by MODIS. In the second example presented in Fig. 3b (16 August 2008), the CALIPSO's aerosol layer product reports 3 aerosol layers. Considering that the only potential aerosol source for the pixel examined is the fire detected by MODIS, the identification of 3 distinct aerosol layers is not consistent with the attenuated backscatter profile reported for the same day and time, where only one layer is visible from the surface up to about 4.5 km (left panel). The slope method (right panel) reports a minimum in the derivative at the height of 4540 m, which coincides with the top of the third layer reported by CALIPSO. Considering our scope to derive smoke injection heights, the most reasonable choice for the Level 2 user in the second example, would be the lower reported layer given that the smoke plume source is at the surface while the elevated second or third layers would be interpreted as advected air masses from remote sources. However, and as the Level 1 profile indicates, a vertical homogeneous distribution is found up to the upper limit of the most elevated layer, thus, the Level 2 user would have eventually used a false injection height from CALIPSO level-2 product, 2 km instead of 4.5 km. Level 2 layer product found to both underestimate or overestimate injection heights retrieved by the slope method in our dataset.

After the demonstration of the cases that CALIPSO Level 2 product fails to estimate top layer height, we here present some basic statistics, also including a comparison between Level 2, Version 2.01 versus Version 3.01 new released products (Fig. 4). The regression analysis between the slope method top layer height and the Level 2, Version 2.01 CALIPSO product (Fig. 4a) depicts that in general the CALIPSO

our dataset, binned in 500 m height intervals is presented in Fig. 5. Labonne et al., (2007), using CALIPSO data for summer 2006 over Eastern Europe found a similar range for the top height of the aerosol layers, ranging from 1.5 to 6 km. This range is the largest globally, as reported in this study.

3.3 Smoke injection in respect to fire intensity and mixing height

Taking into account the large range of injection heights for the studied area, we have tried to investigate the relation between the FRP and the CALIPSO retrieved injection height. The injection heights from CALIPSO used for this comparison are corrected to refer to the surface elevation instead of sea level, for consistency with FRPs which refer to surface fires. This correction could be significant in case of profound orography. However, the exact surface elevation levels of the points included in Fig. 6, taken by the Digital Elevation Model used by CALIPSO at the lidar footprint (GTOPO30 digital elevation map), vary between 0 and 196 m (mean = 125 m, standard deviation = 65 m), and this is rational since we are dealing with agricultural fires initiated in crop fields which are mostly located at non-elevated terrains. Disregarding horizontal transport processes but also the vertical thermal profile of the lower atmosphere (boundary layer and the lower free troposphere), one would expect that the main driver of the fire smoke would be the convection by the fire heat, and thus, higher values of injection heights should be expected for higher FRPs. A simple scatter plot between FRP and injection height (not shown here), showed enhanced dispersion of the values, especially for edge values of FRP (very low or very high). Hence the data are disaggregated into well separated bins so that an adequate number of data pairs are included in each one of the bins (80% of the FRP values in our data set lies in the range 10–40). Following these criteria we have ended up to the following FRP bins: <10, 10–15, 15–20, 20–30, 30–40, >40, each bin represented by the average FRP value and the median injection height (medians are preferred to minimize the influence by injection height outliers). Results are shown in Fig. 6. For the range $10 < \text{FRP} < 40$, a tendency of increasing injection height with FRP is depicted. In all cases the interquartile range of

Smoke injection heights from agricultural burning in Eastern Europe

V. Amiridis et al.

Title Page

Abstract

Introduction

Conclusions

References

Tables

Figures

⏪

⏩

◀

▶

Back

Close

Full Screen / Esc

Printer-friendly Version

Interactive Discussion



Discussion Paper | Discussion Paper | Discussion Paper | Discussion Paper

injection heights per bin is about 1 km, demonstrating our limitations in estimating precise injection height for a given FRP value. However, given that the injection height is a very crucial parameter for smoke dispersion models, the calculated regression line can quite well represent the relation between FRP and injection height, for mid latitudes. The intercept of the line (no fire) is typical of summer boundary layer heights for the area of our interest. The situation is more complex for edge values of FRP. In particular, for $FRP < 10$, we find a disperse range of injection heights mostly between 2 and 4 km. This is probably due to the fact that the smoke injection height, in such low intensity fires, is driven by the meteorological conditions rather than the fire itself. Surprisingly, for $FRP > 40$, the injection height presents a plateau which is below the height for lower FRP. This cannot be explained by horizontal wind speed which shows slow advection for the whole range of FRP values of the current data set, as no significant anti-correlation between horizontal wind speed and injection heights is revealed. It is most likely that MODIS retrievals of FRP in this graph area cannot be entirely trusted due to the presence of dense smoke above the fire area (Kahn et al., 2007).

From the fire cases examined in this paper, we further investigate the range of aerosol top height CALIPSO retrievals by comparing our retrievals with the mixing layer height analyses taken from the ECMWF model, to identify the cases of smoke injection within or above PBL. These comparisons for the studied area and for the fire seasons of the years between 2006 to 2008, are presented in Fig. 7. In both Fig. 7-left and 7-right, near-synchronous ECMWF/CALIPSO measurements are selected. The overpass times of CALIOP and MODIS instruments over the area of study (due to orbit adjustments and geographical area extent) varies between 10:00 and 10:26 UTC for CALIOP/CALIPSO and 10:30 and 10:55 UTC for MODIS/AQUA. According to the abovementioned times, the time difference between the pairs of satellite/model data used in our comparisons, taking into account the use of 12:00 UTC ECMWF analysis data, ranges between 1 h/5 m and 2 h. The only analyses ECMWF BLH fields are from 00:00 and 12:00 UTC. Hence the ECMWF data used for this study refer only to the analyses fields for BLH at 12:00 UTC, which is the closest in time available analyses

Smoke injection heights from agricultural burning in Eastern Europe

V. Amiridis et al.

[Title Page](#)[Abstract](#)[Introduction](#)[Conclusions](#)[References](#)[Tables](#)[Figures](#)[⏪](#)[⏩](#)[◀](#)[▶](#)[Back](#)[Close](#)[Full Screen / Esc](#)[Printer-friendly Version](#)[Interactive Discussion](#)

BLH data to the overpasses. All the other ECMWF products for BLH refer to forecasted fields which are not used in this study.

In the left panel of Fig. 7, all the near-synchronous (12:00 UTC) CALIPSO aerosol top heights and ECMWF mixing layer heights are presented, showing a very good agreement (correlation coefficient equal to 0.952) when the MODIS fire confidence is less than 80%, indicating no fire incident or small scale fires. This indicates that for the small scale fires, the smoke injection height is deterred by BLH of the ambient atmosphere. For MODIS fire confidence greater than 80% (Fig. 7, right panel), the correlation coefficient drops to 0.517. This decrease for the cases with fire confidence greater than 80% may have several plausible reasons listed below:

- a) In presence of strong fire activity the smoke particles can be directly injected well above the PBL height into the free troposphere, and this could be a possible explanation of the greater values of CALIPSO's aerosol top heights compared with those of ECMWF's mixing heights.
- b) The strong fire activity may increase the thermal instability of the ambient lower atmosphere thus inducing an increase of the PBL height, a fact which is not captured by the ECMWF model. This can be due to the fact that the assimilation of the ECMWF model does not take into account the strong updrafts generated by the fires for the calculation of the mixing height.
- c) It could be a combination of both previous explanations.

In Fig. 8, the frequency distribution of the differences between the CALIPSO aerosol top height and ECMWF's estimated mixing height is presented. It is evident that for the 163 cases of fire hot spots examined with fire confidence greater than 80%, the 51.5% of the cases were found to lie within the PBL. For the 48.5% of the cases examined, the smoke has injected directly into the free troposphere according to our calculations. The smoke reached heights above the mixing layer of the order of 0.5 km for 20.8% of the cases, 1 km for 10.4% of the cases and between 1.5 and even 3.0 km for the

Smoke injection heights from agricultural burning in Eastern Europe

V. Amiridis et al.

Title Page

Abstract

Introduction

Conclusions

References

Tables

Figures



Back

Close

Full Screen / Esc

Printer-friendly Version

Interactive Discussion



Discussion Paper | Discussion Paper | Discussion Paper | Discussion Paper | Discussion Paper

Smoke injection heights from agricultural burning in Eastern Europe

V. Amiridis et al.

Title Page

Abstract

Introduction

Conclusions

References

Tables

Figures

⏪

⏩

◀

▶

Back

Close

Full Screen / Esc

Printer-friendly Version

Interactive Discussion



17.3% of the cases. We additionally mention here that the possibility that the layers detected by CALIPSO in higher altitudes might be a result of atmospheric transport than direct injection is not considered strong, since the profiles analyzed show a vertical homogeneity which is mainly attributed to strong convection and corresponding vertical mixing processes. No lifted layers have been observed in the total of 163 profiles examined. In their study for the year 2006, Labonne et al. (2007), reported that the smoke from the fires in Eastern Europe is often contained within the mixing layer, but the authors report also a large number of cases where the smoke extends well above the ECMWF diagnosed top height. Direct injection of smoke in high free-tropospheric altitudes have been reported in the past for biomass burning events in mid and high latitude (Fromm et al., 1998; Jost et al., 2004). However, synoptic transport, including moist convection, cannot be ruled out and a further investigation would require atmospheric transport modeling.

4 Summary and conclusions

The initial injection height of smoke aerosol generated by fires over SW Russia and Eastern Europe during the biomass burning season, for the years between 2006 and 2008, has been investigated using the synergy of CALIPSO and MODIS satellite sensors. CALIPSO derived injection heights for the location of fires (pointed by MODIS fire products) found to be extremely variable, ranging from 1.6 and 5.9 km for the area of our interest. Injection heights for the 163 fires examined, showed a tendency to increase with increased FRP MODIS product which is indicative of the fire intensity, especially in the FRP range between 10 and 40 MW. Edge values of FRP (<10 and >40 MW) did not follow this dependence. For large fires, the MODIS FRP product cannot be entirely trusted due to the presence of dense smoke above the fire area, while less intense fires (FRP<10MW) are not affecting significantly the aerosol top height which is probably driven by thermodynamic boundary layer processes.

Smoke injection heights from agricultural burning in Eastern Europe

V. Amiridis et al.

Title Page

Abstract

Introduction

Conclusions

References

Tables

Figures

⏪

⏩

◀

▶

Back

Close

Full Screen / Esc

Printer-friendly Version

Interactive Discussion



For the analysis of the smoke injection height in relation to the mixing layer thickness, ECMWF model estimations of the mixing layer height have been used for the hot spots analyzed in this paper. For the cases of fires with low intensity (or no fires), corresponding to fire confidence lower than 80%, data strongly support that biomass burning plumes are injected within the mixing layer, as diagnosed by the ECMWF short-range forecast. However, for the 163 cases of fires under study in this paper (with fire confidences greater than 80% according to MODIS), data indicated also cases when smoke penetrates in the free troposphere. Approximately 50% of the cases examined showed that the smoke reached heights above the mixing layer. The atmospheric transport of smoke from distant sources for the cases reported here is not considered strong, since the CALIPSO profiles analyzed showed a vertical homogeneity which is mainly attributed to strong convection above the fire locations and corresponding vertical mixing processes. However, the local direct injection of smoke at free tropospheric heights can have large impact in longer distances. Similar arguments considering the use of CALIPSO vertical homogeneity to attribute the smoke presence to local fires can be relevant for other areas with large fires (e.g. Amazon, Africa, and Australia).

CALIPSO lidar show a lot of advantages for smoke injection height studies. Future work including the synergy of CALIPSO and MISR sensors could be a potential method for most accurate geometrical characterization of smoke plumes. Additional modeling tools for atmospheric transport calculations, including moist convection, can be synergistically used to provide parameterizations of biomass burning plumes in general circulation models.

Acknowledgements. The research work was financially supported by the European Commission's research project: Monitoring Atmospheric Composition and Climate (MACC) – Grant agreement no.: 218 793, 7th Framework Programme – Theme 9: Space and by the EU-FP6 EARLINET-ASOS project (RICA-025991). SK would like to acknowledge Marie Curie project ACI-UV, PERG05-GA-2009-247492.

References

- Amiridis, V., Balis, D. S., Kazadzis, S., Bais, A., Giannakaki, E., Papayannis, A., and Zerefos, C.: Four-year aerosol observations with a Raman lidar at Thessaloniki, Greece, in the framework of European Aerosol Research Lidar Network (EARLINET), *J. Geophys. Res.*, 110, D21203, doi:10.1029/2005JD006190, 2005.
- Amiridis, V., Balis, D. S., Giannakaki, E., Stohl, A., Kazadzis, S., Koukouli, M. E., and Zanis, P.: Optical characteristics of biomass burning aerosols over Southeastern Europe determined from UV-Raman lidar measurements, *Atmos. Chem. Phys.*, 9, 2431–2440, doi:10.5194/acp-9-2431-2009, 2009.
- Balis, D., Amiridis, V., Zerefos, C., Gerasopoulos, E., Andreae, M. O., Zanis, P., Kazantzidis, A., Kazadzis, S., and Papayannis, A.: Raman lidar and sunphotometric measurements of aerosol optical properties over Thessaloniki, Greece, during a biomass burning episode, *Atm. Env.*, 37(32), 4529-4538, 2003
- Colarco, P. R., Schoeberl, M. R., Doddridge, B. G., Marufu, L. T., Torres, O., and Welton, E. J.: Transport of smoke from Canadian forest fires to the surface near Washington, D. C.: Injection height, entrainment, and optical properties, *J. Geophys. Res.*, 109, D06203, doi:10.1029/2003JD004248, 2004.
- Diner, D. J., Beckert, J., Reilly, T., Bruegge, C., Conel, J., Kahn, R., Martonchik, J., Ackerman, T., Davies, R., Gerstl, S., Gordon, H., Muller, J.-P., Myneni, R., Sellers, P., Pinty, B., and Verstraete, M., Multi-angle Imaging SpectroRadiometer (MISR) instrument description and experiment overview, *IEEE Trans. Geosci. Remote Sens.*, 36, 1072–1087, 1998.
- Dirksen, R. J., Folkert Boersma, K., de Laat, J., Stammes, P., van der Werf, G. R., Val Martin, M., and Kelder, H. M.: An aerosol boomerang: Rapid around-the-world transport of smoke from the December 2006 Australian forest fires observed from space, *J. Geophys. Res.*, 114, D21201, doi:10.1029/2009JD012360, 2009.
- ECMWF: IFS Documentation – CY33r1. Part II: Data Assimilation. European Center for Medium-Range Weather Forecasts, Shinfield Park, Reading, England, 160 pp, (<http://www.ecmwf.int/research/ifsdocs/CY33r1/ASSIMILATION/IFSPart2.pdf>), 2009a.
- ECMWF: IFS Documentation – CY33r1. Part IV: Physical Processes. European Center for Medium-Range Weather Forecasts, Shinfield Park, Reading, England, 162 pp, (<http://www.ecmwf.int/research/ifsdocs/CY33r1/PHYSICS/IFSPart4.pdf>), 2009b.
- Flamant, C., Pelon, J., Flamant, P., and Durand, P.: Lidar determination of the entrainment

ACPD

10, 19247–19276, 2010

Smoke injection heights from agricultural burning in Eastern Europe

V. Amiridis et al.

Title Page

Abstract

Introduction

Conclusions

References

Tables

Figures

⏪

⏩

◀

▶

Back

Close

Full Screen / Esc

Printer-friendly Version

Interactive Discussion

Smoke injection heights from agricultural burning in Eastern Europe

V. Amiridis et al.

Title Page

Abstract

Introduction

Conclusions

References

Tables

Figures

◀

▶

◀

▶

Back

Close

Full Screen / Esc

Printer-friendly Version

Interactive Discussion



zone thickness at the top of the unstable marine, atmospheric boundary layer, *Boundary Layer Meteorol.*, 83, 247–284, 1997.

Fotiadi, A., Hatzianastassiou, N., Drakakis, E., Matsoukas, C., Pavlakis, K. G., Hatzidimitriou, D., Gerasopoulos, E., Mihalopoulos, N., and Vardavas, I.: Aerosol physical and optical properties in the Eastern Mediterranean Basin, Crete, from Aerosol Robotic Network data, *Atmos. Chem. Phys.*, 6, 5399–5413, doi:10.5194/acp-6-5399-2006, 2006.

Freitas, S. R., Longo, K. M., Chatfield, R., Latham, D., Silva Dias, M. A. F., Andreae, M. O., Prins, E., Santos, J. C., Gielow, R., and Carvalho Jr., J. A.: Including the sub-grid scale plume rise of vegetation fires in low resolution atmospheric transport models, *Atmos. Chem. Phys.*, 7, 3385–3398, doi:10.5194/acp-7-3385-2007, 2007.

Fromm, M., Alfred, J., Hoppel, K., Hornstein, J., Bevilacqua, R., Shettle, E., Servranckx, R., Li, Z., and Stocks, B.: Observations of boreal forest fire smoke in the stratosphere by POAM III, SAGE II, and lidar in 1998, *Geophys. Res. Lett.*, 27, 1407–1410, 1998.

Gerasopoulos, E., Andreae, M. O., Zerefos, C. S., Andreae, T. W., Balis, D., Formenti, P., Merlet, P., Amiridis, V., and Papastefanou, C.: Climatological aspects of aerosol optical properties in Northern Greece, *Atmos. Chem. Phys.*, 3, 2025–2041, doi:10.5194/acp-3-2025-2003, 2003.

Gerasopoulos, E., Kouvarakis, G., Babasakalis, P., Vrekoussis, M., Putaud, J. P., and Mihalopoulos, N.: Origin and variability of particulate matter (PM₁₀) mass concentrations over the eastern Mediterranean, *Atm. Env.*, 40, 4679–4690, 2006.

Giglio, L., Descloitres, J., Justice, C. O., and Kaufman, Y. J.: An enhanced contextual fire detection algorithm for MODIS, *Remote Sens. Environ.*, 87, 273–282, doi:10.1016/S0034-4257(03)00184-6, 2003.

Haseler, J., Early-delivery suite, ECMWF Newsletter No 101, 21–30 pp, 2004.

Ichoku, C., Giglio, L., Wooster, M. J., and Remer, L. A.: Global characterization of biomass-burning patterns using satellite measurements of Fire Radiative Energy. *Remote Sens. Environ.*, 112, 2950–2962, 2008.

Jost, H.-J., Drdla, K., Stohl, A., et al.: In-situ observations of mid-latitude forest fire plumes deep in the stratosphere, *Geophys. Res. Lett.*, 31, L11101, doi:10.1029/2003GL019253, 2004.

Kahn, R. A., Chen, Y., Nelson, D. L., Leung, F.-Y., Li, Q., Diner, D. J., and Logan, J. A.: Wildfire Smoke Injection Heights—Two Perspectives from Space, *Geophys. Res. Lett.*, 35, L04809, doi:10.1029/2007GL032165, 2008.

Kahn, R. A., Li, W.-H., Moroney, C., Diner, D. J., Martonchik, J. V., and Fishbein, E.: Aerosol source plume physical characteristics from space-based multi-angle imaging, *J. Geophys.*

Smoke injection heights from agricultural burning in Eastern Europe

V. Amiridis et al.

Title Page

Abstract

Introduction

Conclusions

References

Tables

Figures

◀

▶

◀

▶

Back

Close

Full Screen / Esc

Printer-friendly Version

Interactive Discussion



Res., 112, D11205, doi:10.1029/2006JD007647, 2007.

Kaimal, J. C., Abshire, N. L., Chadwick, R. B., Decker, M. T., Hooke, W. H., Kropfli, R. A., Neff, W. D., Pasqualucci, F., and Hildebrand, P. H.: Estimating the depth of the daytime convective boundary layer, *J. Appl. Meteorol.*, 21, 1123–1129, 1982.

5 Kazadzis, S., Bais, A., Amiridis, V., Balis, D., Meleti, C., Kouremeti, N., Zerefos, C. S., Rapsomanikis, S., Petrakakis, M., Kelesis, A., Tzoumaka, P., and Kelektsoglou, K.: Nine years of UV aerosol optical depth measurements at Thessaloniki, Greece, *Atmos. Chem. Phys.*, 7, 2091–2101, doi:10.5194/acp-7-2091-2007, 2007.

10 Korontzi, S., McCarty, J., Loboda, T., Kumar, S., and Justice, C.: Global distribution of agricultural fires in croplands from 3 years of Moderate Resolution Imaging Spectroradiometer (MODIS) data, *Global Biogeochem. Cycles*, 20, GB2021, doi:10.1029/2005GB002529, 2006.

15 Labonne, M., Breon, F.-M., and Chevallier, F.: Injection height of biomass burning aerosols as seen from a spaceborne lidar, *Geophys. Res. Lett.*, 34, L11806, doi:10.1029/2007GL029311, 2007.

Lelieveld, J., Berresheim, H., Borrmann, S., Crutzen, P. J., et al.: Global air pollution crossroads over the Mediterranean, *Science* 298, 794–799, 2002.

Menut, L., Flamant, C., Pelon, J., and Flamant, P.: Urban boundary layer height determination from lidar measurements over the Paris area, *Appl. Opt.*, 38, 945–954, 1999.

20 Mims, S. R., Kahn, R. A., Moroney, C. M., Gaitley, B. J., Nelson, D. L., and Garay, M. J.: MISR Stereo Heights of Grassland Fire Smoke Plumes in Australia, *IEEE Transactions on Geoscience and Remote Sensing*, 48, 25–35 pp, No. 1, 2010.

Pal, S. R., Steinbrecht, W., and Carswell, A. I.: Automated method for lidar determination of cloud base height and vertical extent, *Appl. Optics*, 31, 1488–1494, 1992.

25 Persson A. and Grazzini, F.: User Guide to ECMWF forecast products. *Meteorological Bulletin M3.2*. European Center for Medium-Range Weather Forecasts, Shinfield Park, Reading, England, 154 pp., 2005.

Troen, I. and Mahrt, L.: A simple model of the atmospheric boundary layer; sensitivity to surface evaporation, *Boundary-Layer Meteorol.*, 37, 129–148, 1986.

30 Val Martin, M., Logan, J. A., Kahn, R. A., Leung, F.-Y., Nelson, D. L., and Diner, D. J.: Smoke injection heights from fires in North America: analysis of 5 years of satellite observations, *Atmos. Chem. Phys.*, 10, 1491–1510, doi:10.5194/acp-10-1491-2010, 2010.

Vaughan, M. A., Young, S. A., Winker, D., Powell, K., Omar, A., Liu, Z., Hu, Y., Hostetler, C.:

Smoke injection heights from agricultural burning in Eastern Europe

V. Amiridis et al.

Title Page

Abstract

Introduction

Conclusions

References

Tables

Figures

⏪

⏩

◀

▶

Back

Close

Full Screen / Esc

Printer-friendly Version

Interactive Discussion



Fully automated analysis of space-based lidar data: an overview of the CALIPSO retrieval algorithms and data products, Proc. SPIE, 5575,16, doi:10.1117/12.572024, 2004.

Winker, D., Hostetler, C., and Hunt, W.: CALIOP: The CALIPSO Lidar, Proc. 22nd International Laser Radar Conference (ESASP 561), Matera, Italy, 941–944, 2004.

5 Winker, D., Vaughan, M., and Hunt, W.: The CALIPSO mission and initial results from CALIOP, Proc. SPIE, 6409, 640902, doi:10.1117/12.698003, 2006.

Winker D. M., Hunt, W. H., McGill, M. J., et al.: Initial performance assessment of CALIOP, Geophys. Res. Lett., 34, L19803, doi:10.1029/2007GL030135, 2007.

10 Winker, D., Vaughan, M., Omar, A., Hu, Y., Powell, K., Liu, Z., Hunt, W., Young, S.: Overview of the CALIPSO Mission and CALIOP Data Processing Algorithms, J. Atm. Ocean. Tech., 26, 2310–2323, 2009.

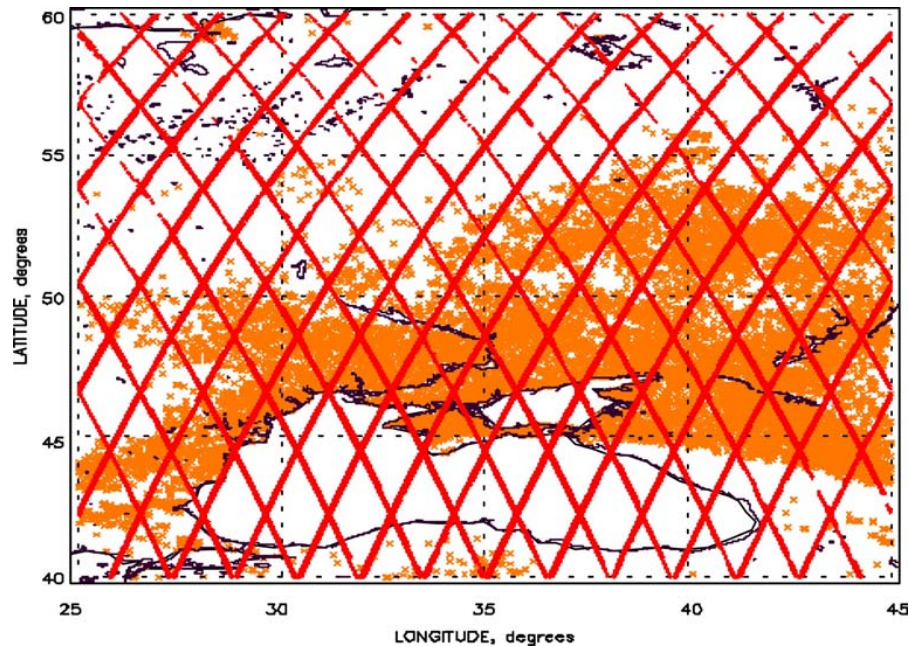


Fig. 1. Active fires as seen by MODIS during July and August 2006, 2007, 2008 for the Western Russian and Eastern Europe area. CALIPSO overpasses during the same time period are superimposed.

Smoke injection heights from agricultural burning in Eastern Europe

V. Amiridis et al.

[Title Page](#)

[Abstract](#) [Introduction](#)

[Conclusions](#) [References](#)

[Tables](#) [Figures](#)

[◀](#) [▶](#)

[◀](#) [▶](#)

[Back](#) [Close](#)

[Full Screen / Esc](#)

[Printer-friendly Version](#)

[Interactive Discussion](#)



**Smoke injection
heights from
agricultural burning
in Eastern Europe**

V. Amiridis et al.

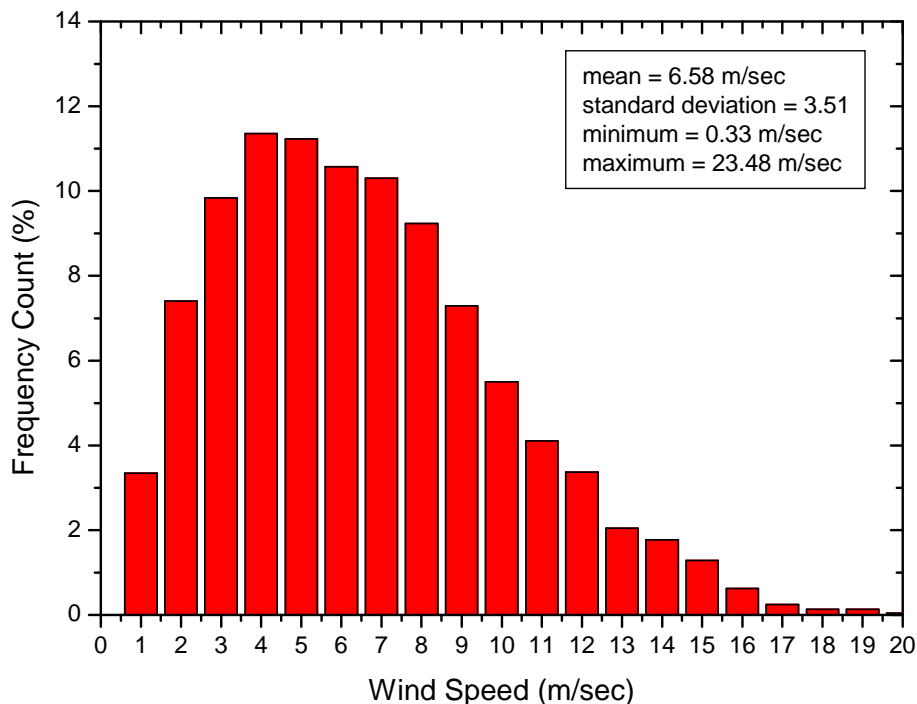


Fig. 2. Frequency distribution of ECMWF wind speed analyses at 850 hPa for the times and locations of fires under study over the Western Russian and Eastern Europe during July and August 2006, 2007, 2008.

[Title Page](#)[Abstract](#)[Introduction](#)[Conclusions](#)[References](#)[Tables](#)[Figures](#)[◀](#)[▶](#)[◀](#)[▶](#)[Back](#)[Close](#)[Full Screen / Esc](#)[Printer-friendly Version](#)[Interactive Discussion](#)

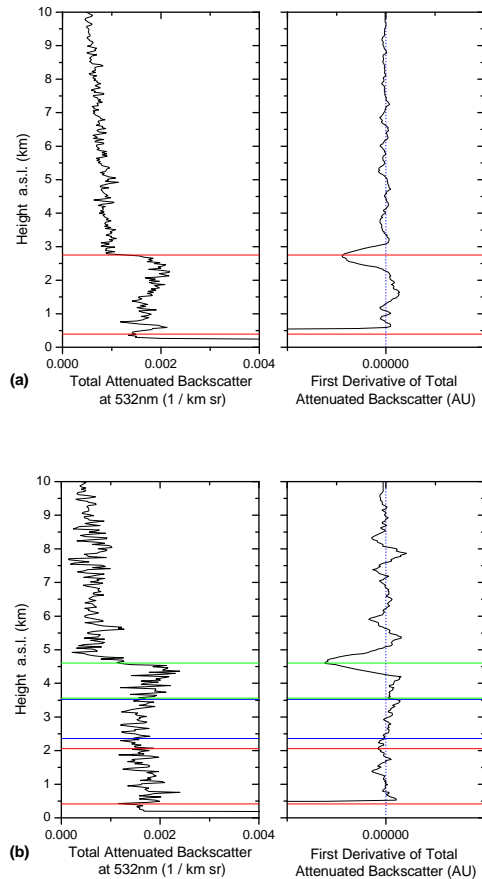


Fig. 3. Examples of CALIPSO Level-1 attenuated backscatter profiles at 532 nm and the corresponding Level-2 aerosol layer product (left panels) and the profiles of the corresponding first derivative of the attenuated backscatter coefficient (right panels) at 15 August 2006 (upper panels) and 16 August 2008 (lower panels).

Smoke injection heights from agricultural burning in Eastern Europe

V. Amiridis et al.

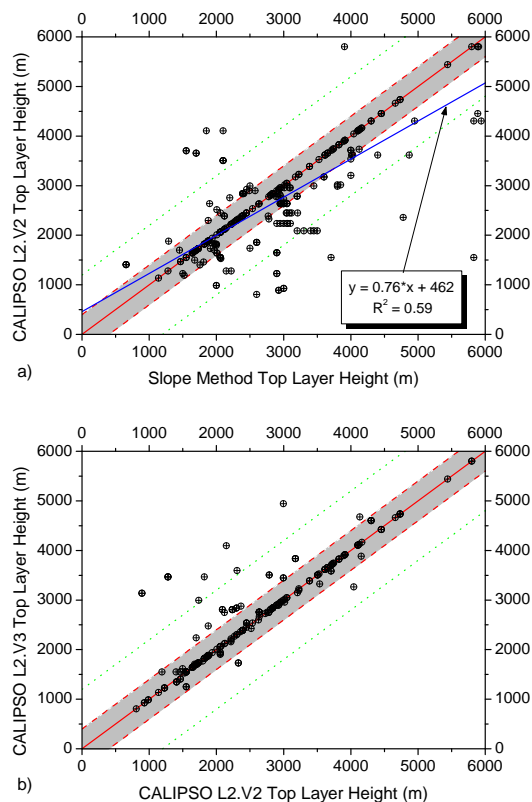


Fig. 4. (a) Scatter plot of aerosol top layer heights derived from CALIPSO Level 2, Version 2.01 product versus the slope method. (b) Comparison between Version 2.01 and Version 3.01 of the Level 2 CALIPSO layer product. The red continuous lines represent the 1:1 relationship while the regression line is shown in blue. The gray area limited by the red dashed lines represents the window frame of 400 m (WF400) applied for the slope method and the green dotted lines accounts for 3 WF400.

Title Page

Abstract

Introduction

Conclusions

References

Tables

Figures

◀

▶

◀

▶

Back

Close

Full Screen / Esc

Printer-friendly Version

Interactive Discussion

Smoke injection heights from agricultural burning in Eastern Europe

V. Amiridis et al.

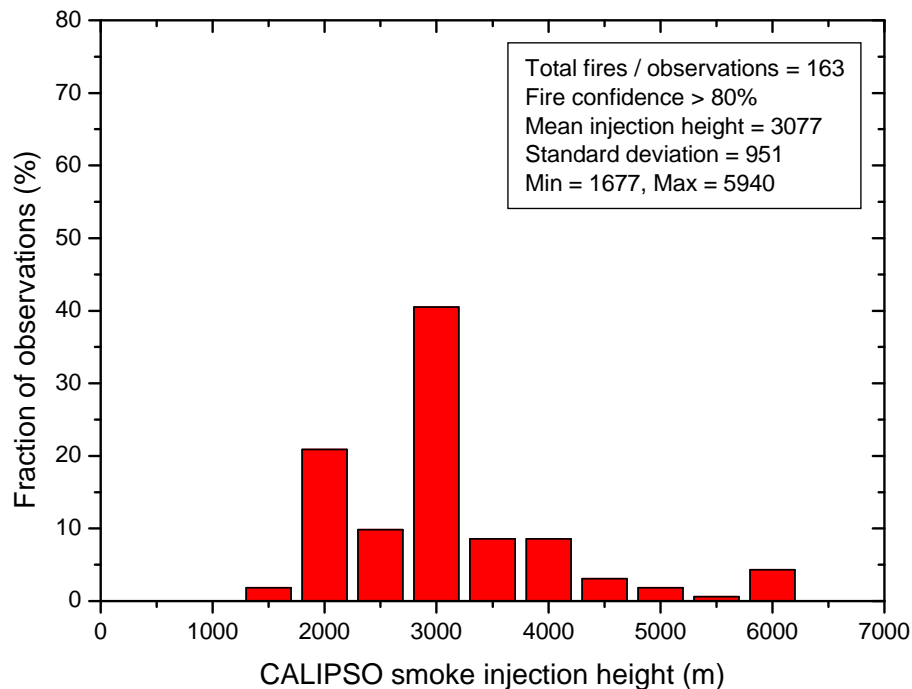


Fig. 5. Frequency distribution of the aerosol top height binned in 500 m height intervals, as retrieved by CALIPSO over the Western Russian and Eastern Europe during July and August 2006, 2007, 2008.

[Title Page](#)[Abstract](#)[Introduction](#)[Conclusions](#)[References](#)[Tables](#)[Figures](#)[⏪](#)[⏩](#)[◀](#)[▶](#)[Back](#)[Close](#)[Full Screen / Esc](#)[Printer-friendly Version](#)[Interactive Discussion](#)

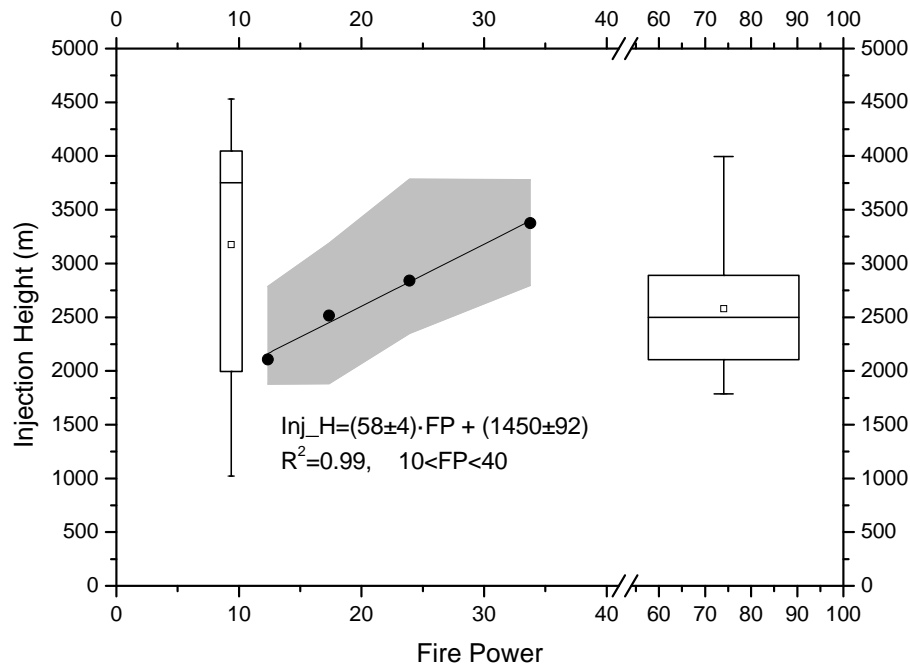


Fig. 6. Scatter-plot of binned data of Fire Power versus smoke Injection Height. For the range $10 < \text{FP} < 40$, each point represents the average FP versus the median injection height, while the gray area represents the interquartile range of the injection heights distribution. The solid line is the linear regression line for the range $10 < \text{FP} < 40$ (values after \pm are the standard error of the estimated parameter). For FP range < 10 and > 40 , whisker boxes are shown: the box height is limited between the 1st and the 3rd quartiles, the internal line is the median while the open square stands for the average, the error bars are the minimum and maximum values of injection height. The width of the box is proportional to the standard deviation of the FP bin values.

Smoke injection heights from agricultural burning in Eastern Europe

V. Amiridis et al.

Title Page

Abstract Introduction

Conclusions References

Tables Figures

⏪ ⏩

◀ ▶

Back Close

Full Screen / Esc

Printer-friendly Version

Interactive Discussion



Smoke injection heights from agricultural burning in Eastern Europe

V. Amiridis et al.

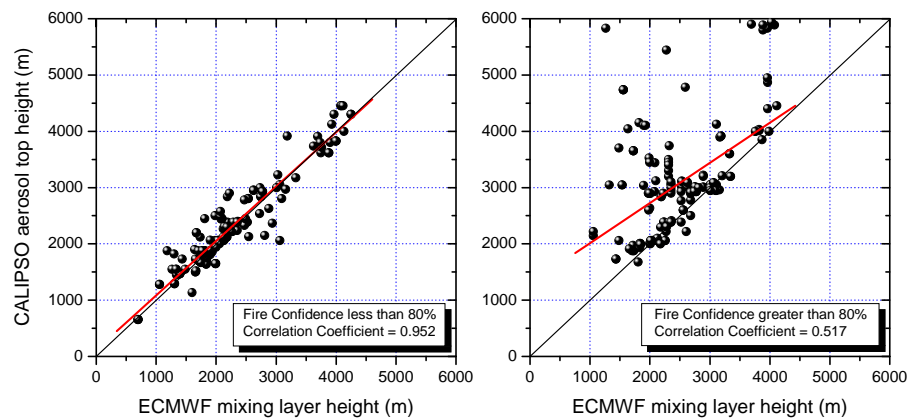


Fig. 7. Comparison of aerosol top height derived by CALIPSO with mixing layer height from ECMWF model for fire confidence less than 80% (left panel) and greater than 80% (right panel).

[Title Page](#)[Abstract](#)[Introduction](#)[Conclusions](#)[References](#)[Tables](#)[Figures](#)[◀](#)[▶](#)[◀](#)[▶](#)[Back](#)[Close](#)[Full Screen / Esc](#)[Printer-friendly Version](#)[Interactive Discussion](#)

Smoke injection heights from agricultural burning in Eastern Europe

V. Amiridis et al.

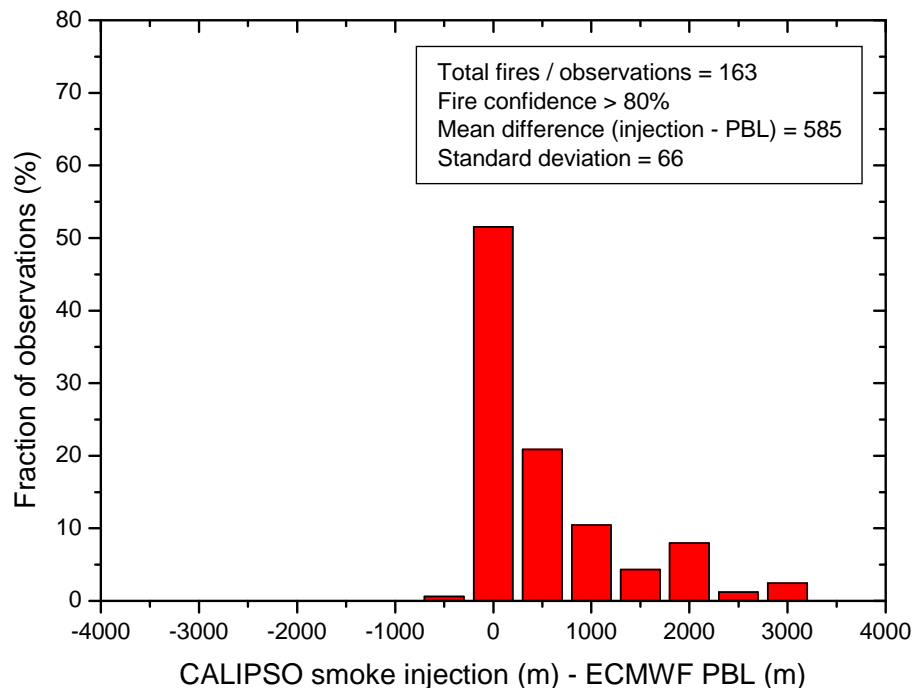


Fig. 8. Frequency distribution of the differences between CALIPSO derived smoke injection height and ECMWF's mixing layer height for the cases with fire confidence greater than 80%.

[Title Page](#)[Abstract](#)[Introduction](#)[Conclusions](#)[References](#)[Tables](#)[Figures](#)[◀](#)[▶](#)[◀](#)[▶](#)[Back](#)[Close](#)[Full Screen / Esc](#)[Printer-friendly Version](#)[Interactive Discussion](#)